

University of Toronto

Faculty of Applied Science and Engineering

ECE422H1 Radio and Microwave Wireless Systems

Lab 2: Antenna Arrays

Prepared by Aurora Nowicki & Deniz Uzun

PRA0101 - February 7, 2024

2 Network Analyzer Calibration

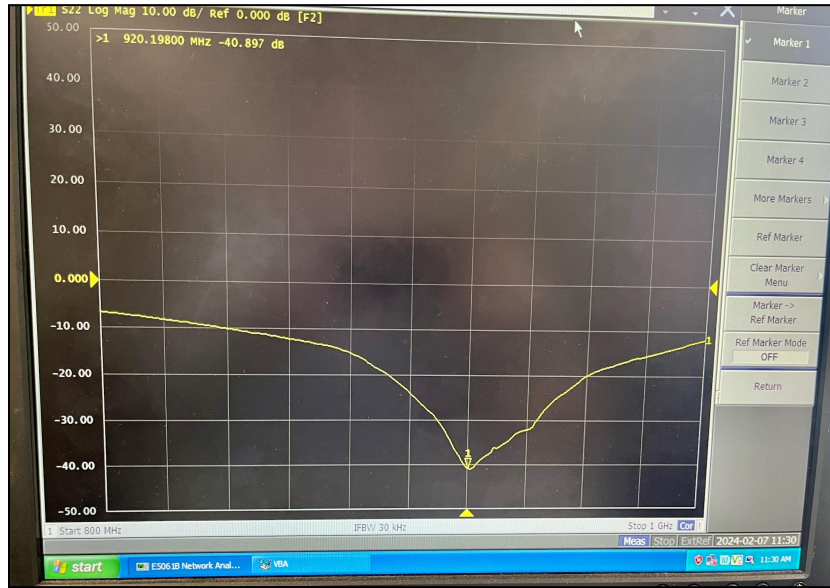


Figure 1: Frequency at which Yagi antenna operates

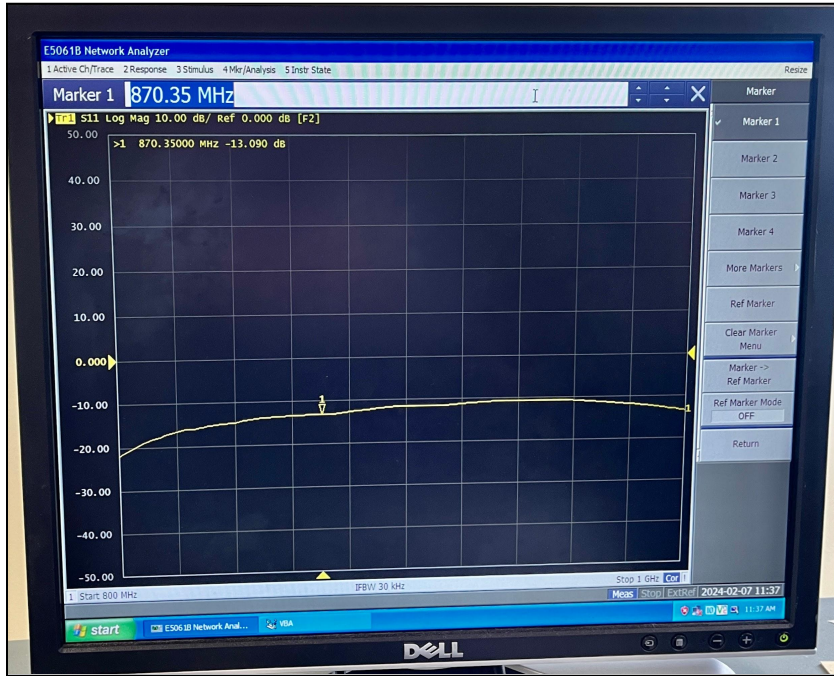


Figure 2: Frequency at which half-wave dipole antenna operates

From *Figure 1 and 2*, we determine the resonant frequency at which the Yagi antenna operates to be 920 MHz and suitable compatible resonant frequency at which the half-wave dipole antenna will operate to be 870 MHz.

3 Two-Element Linear Array

3.1 Two-Element Array with $d = \lambda/2$ and $\alpha = 0^\circ$

9-11. Record the S_{21} value measured by the network analyzer.

Table 1: S_{21} (dB) measurements for the two-element array with $d = \lambda/2$ and $\alpha = 0^\circ$ with respect to various angles of rotation in 15 degree increments

Angle (in degrees)	S_{21} (dB)
0	-41
15	-33
30	-28
45	-26
60	-25
75	-24.1
90	-25
105	-25.3
120	-28
135	-30.1
150	-33.5
165	-34
180	-38
195	-35.1
210	-33.6
225	-32
240	-33
255	-32
270	-33
285	-32
300	-34
315	-39
330	-37.8
345	-38

Plot the pattern and compare it to the theoretical pattern expected from a half-wave dipole array in this configuration.

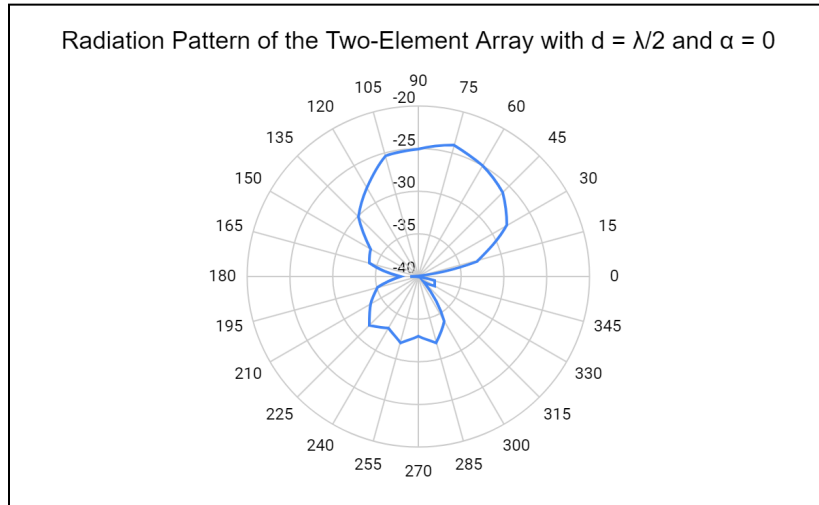


Figure 3: Co-polarized radiation pattern of the two-element antenna array with $d = \lambda/2$ and $\alpha = 0^\circ$, plotted as polar chart using the S21 (dB) measurements in Table 1

Theoretical Pattern

$$\text{Total Pattern } (F) = \frac{\cos(\frac{\pi}{2}\cos\theta)}{\sin\theta} \cos\left(\frac{kd}{2}\cos\theta\right) = \frac{\cos(\frac{\pi}{2}\cos\theta)}{\sin\theta} \cos\left(\frac{\pi}{2}\cos\theta\right)$$

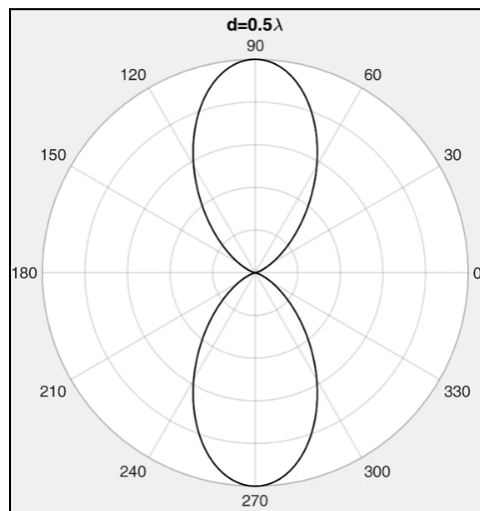


Figure 4: Theoretical radiation pattern of the two-element antenna array with $d = \lambda/2$ and $\alpha = 0^\circ$ [1]

Nulls are expected to occur when $\cos(\frac{\pi}{2}\cos\theta) = 0$ so $\frac{\pi}{2}\cos\theta = \pm \frac{\pi}{2}, \pm \frac{3\pi}{2}$, at $\theta = 0^\circ, \pm 180^\circ$.

The radiation pattern in Figure 3, has a main lobe along the 90° and nulls along the 0° and 180° which is consistent with our theoretical expectations from Figure 4.

3.2 Two-Element Array with $d = \lambda$ and $\alpha = 0^\circ$

Repeat the procedure in Section 3.1 but change the array spacing to $d = \lambda$. How many lobes do you observe in the pattern? Compare measurements to theory and comment on what you observe.

Table 2: S_{21} (dB) measurements for the two-element array with $d = \lambda$ and $\alpha = 0^\circ$ with respect to various angles of rotation in 15 degree increments

Angle (in degrees)	S_{21} (dB)
0	-28
15	-27.7
30	-28
45	-39
60	-33
75	-25.8
90	-25
105	-26
120	-33
135	-42
150	-33.4
165	-30.2
180	-30
195	-26.8
210	-27.7
225	-35
240	-35
255	-27
270	-29
285	-40
300	-34
315	-26.7
330	-26.5
345	-27

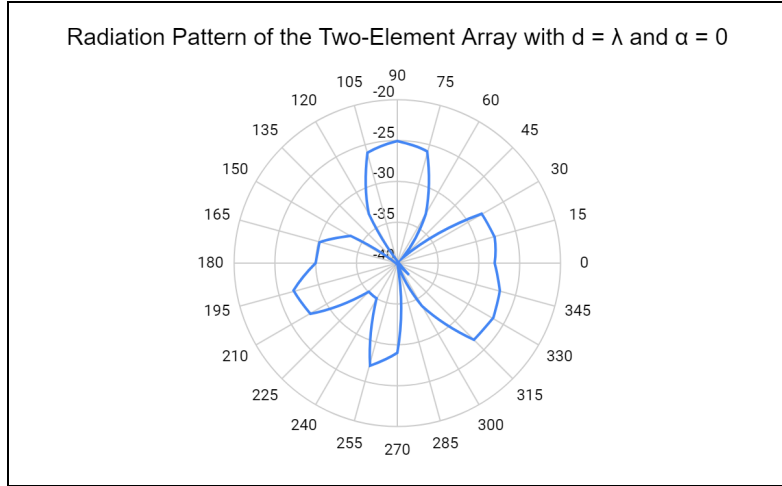


Figure 5: Co-polarized radiation pattern of the two-element antenna array with $d = \lambda$ and $\alpha = 0^\circ$, plotted as polar chart using the S21 (dB) measurements in Table 2

Theoretical Pattern

$$\text{Total Pattern} = \frac{\cos(\frac{\pi}{2}\cos\theta)}{\sin\theta} \cos\left(\frac{kd}{2}\cos\theta\right) = \frac{\cos(\frac{\pi}{2}\cos\theta)}{\sin\theta} \cos(\pi\cos\theta)$$

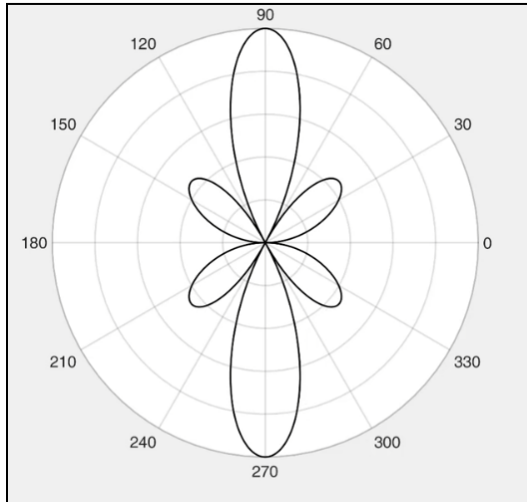


Figure 6: Theoretical total radiation pattern of the two-element antenna array with $d = \lambda$ and $\alpha = 0^\circ$ [1]

Nulls are expected to occur when $\cos(\pi\cos\theta) = 0$ so $\pi\cos\theta = \pm\frac{\pi}{2}, \pm\frac{3\pi}{2}$ at $\theta = \pm 60^\circ, \pm 120^\circ$. From Figure 5, we observe 3 lobes in the radiation pattern: 1 main lobe and 2 side lobes where θ ranges from 0 to 180 degrees. Nulls occur between the additive points in the pattern, whenever contributions from both sources are 180° out of phase. In our measurements nulls occur at around $\theta = +45^\circ, +135^\circ, +240^\circ$ and $+285^\circ$, which are quite close to our expectations. The error could be attributed to imprecise measurements of rotation degrees during the experiment. As expected, we observe the main lobe along $\theta = +90^\circ$ creating a broadside radiation pattern. We additionally observe 2 significant side lobes, one on each side of the main lobe, symmetrically located, just before the nulls.

3.3 Two-Element Array with $d = \lambda/4$ and $\alpha = 90^\circ$

Repeat the procedure in Section 3.1 but change the array spacing to $d = \lambda/4$. To introduce the 90° degree phase difference between elements, use a quadrature hybrid (with the isolated port terminated in a 50Ω load to feed the array).

Table 3: S_{21} (dB) measurements for the two-element array with $d = \lambda/4$ and $\alpha = 90^\circ$ with respect to various angles of rotation in 15 degree increments

Angle (in degrees)	S_{21} (dB)
0	-47
15	-31
30	-30.7
45	-34
60	-38
75	-33.5
90	-31
105	-30
120	-29.5
135	-31
150	-29
165	-28.8
180	-30
195	-29
210	-28
225	-24.5
240	-24.5
255	-25.7
270	-27
285	-32
300	-34
315	-37
330	-33
345	-38

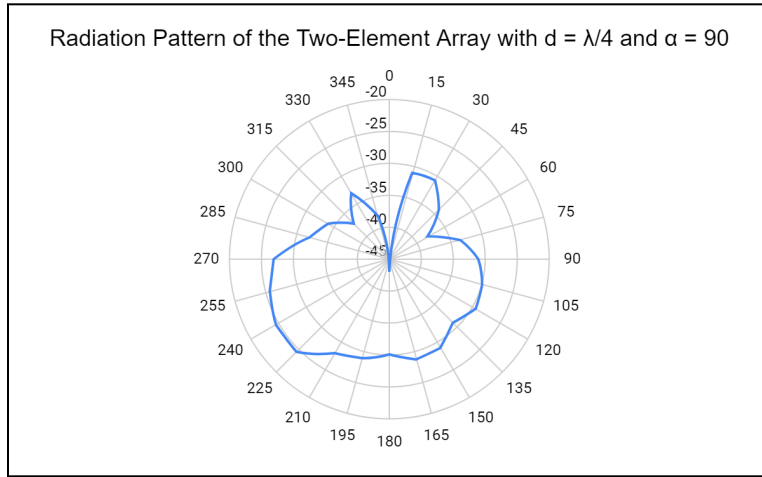


Figure 7: Co-polarized radiation pattern of the two-element antenna array with $d = \lambda/4$ and $\alpha = 90^\circ$, plotted as polar chart using the S21 (dB) measurements in Table 3

$$\text{Total Pattern} = \frac{\cos(\frac{\pi}{2}\cos\theta)}{\sin\theta} \cos\left(\frac{kd}{2}\cos\theta + \beta\right) = \frac{\cos(\frac{\pi}{2}\cos\theta)}{\sin\theta} \cos\left(\frac{\pi}{4}\cos\theta + 90^\circ\right)$$

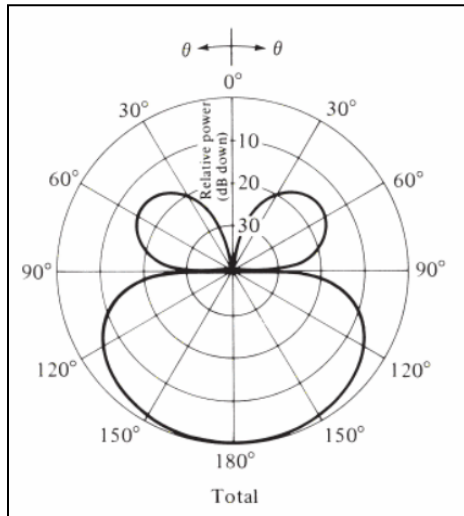


Figure 8: Theoretical radiation pattern of the two-element antenna array of infinitesimal horizontal dipoles with $d = \lambda/4$ and $\alpha = 90^\circ$ [2]

\cos(\frac{\pi}{4}\cos\theta + 90^\circ) = 0 so $\frac{\pi}{4}\cos\theta + \frac{\pi}{2} = \pm \frac{\pi}{2}$ at $\theta = 90^\circ$

The null at 0° is introduced by the array factor. Our results in Figure 7 mostly align with the theoretical expectation, in Figure 8. Although we cannot observe the nulls at 90° , there are dips in the plot around 60° and 315° (-45°). This error could be attributed to measurement errors such as imprecise measurement of the angle and the signal. (Note: Figure 7 has been plotted with a different angle convention than other figures, mainly to match the reference in Figure 8.)

4 Four-Element Linear Array with $d = \lambda/2$

4.1 Uniform Array ($\alpha = 0^\circ$)

Table 4: S_{21} (dB) measurements for the four-element array with $d = \lambda/2$ and $\alpha = 0^\circ$ with respect to various angles of rotation in 15 degree increments

Angle (in degrees)	S_{21} (dB)
0	-37.5
15	-34.5
30	-31.2
45	-28.5
60	-30
75	-25.7
90	-23
105	-31
120	-33
135	-29
150	-30
165	-29.7
180	-30
195	-34
210	-33
225	-32.6
240	-31.7
255	-31
270	-26
285	-28.5
300	-33
315	-30
330	-28
345	-35

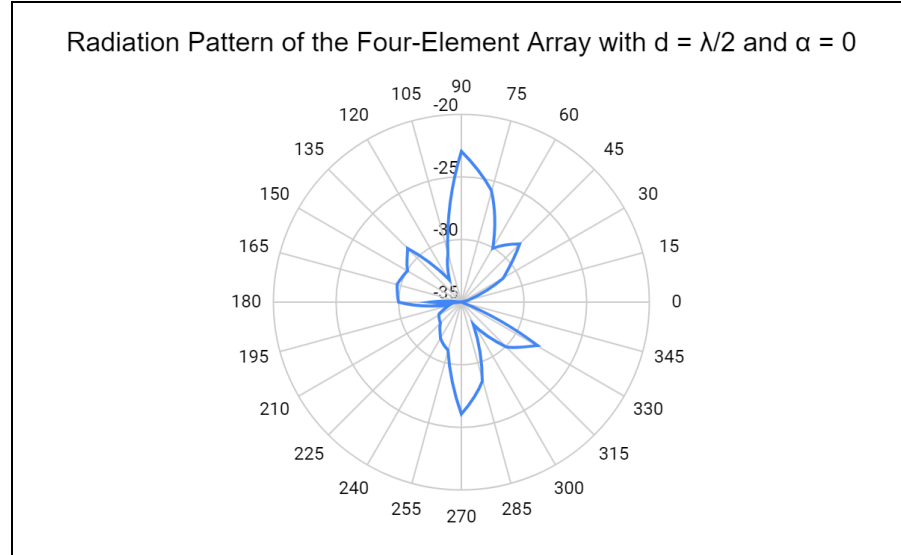


Figure 9: Co-polarized radiation pattern of the four-element uniform antenna array with $d = \lambda/2$ and $\alpha = 0^\circ$, plotted as polar chart using the S21 (dB) measurements in Table 4

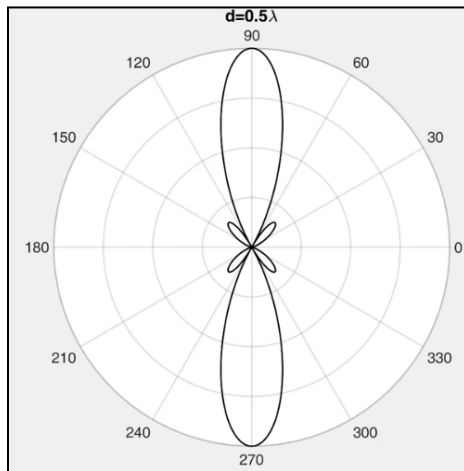


Figure 10: Theoretical radiation pattern of the four-element antenna array with $d = \lambda/2$ and $\alpha = 0^\circ$ [1]

$$\Psi = kdcos(\theta) = \frac{2\pi}{\lambda} \frac{\lambda}{2} cos(\theta) = \pi cos(\theta)$$

Nulls occur at $\frac{N\Psi}{2} = \pm n\pi$ where $N = 4$ so that $\Psi = \pm \frac{n\pi}{2} = \pi cos(\theta)$

The radiation pattern in *Figure 9*, has a main lobe around 90° as expected in comparison to *Figure 10*. We observe dips (nulls) along the 60° and 120° , creating 2 sidelobes on either side of the main lobe, which is consistent with our theoretical expectations from *Figure 12*.

Compare the pattern to theoretical expectations.

With a theoretical 4 element linear array with $\frac{\lambda}{2}$ separation and same phase shift, the theoretical expression we expect can be simplified with the parallel ray approximation. We can say

$R_n = r - \frac{nS}{2} \cos\theta$, with $S = \frac{\lambda}{2}$, $n = -3, -1, 1, 3$ and θ the independent variable. Orienting each dipole parallel to the x-axis, we can thus define the meter stick aligning the dipoles as the z-axis, since we want the rotation of the meter stick parallel to the floor as a change in theta.

Since we have 4 elements and each is a half-wave dipole, the element factor of the array is the original field of a single half-wave dipole aligned along the x-axis. The resulting electric field is then multiplied by the array factor, which results from summing the phase terms of the 4-element array. In our case, AF arises from the approximation of $\exp(-jkR) = \exp(-jk(r + R_n))$, where R_n =distance of each dipole from the origin. Simplifying the exponential terms using Euler's formula and substituting $S = \frac{\lambda}{2}$, we get the following:

$$AF = 2\cos(k \frac{\lambda}{4} \cos\theta) + 2\cos(k \frac{3\lambda}{4} \cos\theta) = 2\cos(\frac{\pi}{2} \cos\theta) + 2\cos(\frac{3\pi}{2} \cos\theta)$$

By pattern multiplication, we can see the difference between the field produced by a single dipole and one produced by 4 dipoles.

In the x-z plane ($\phi = \text{const.}$):

Plot of the normalized element pattern of a $\frac{\lambda}{2}$ dipole parallel to x-axis =>

$$\frac{\cos(\frac{\pi}{2} \sin\theta \cos\phi)}{1 - (\sin^2 \theta \cos^2 \phi)} \cos\theta \cos\phi :$$

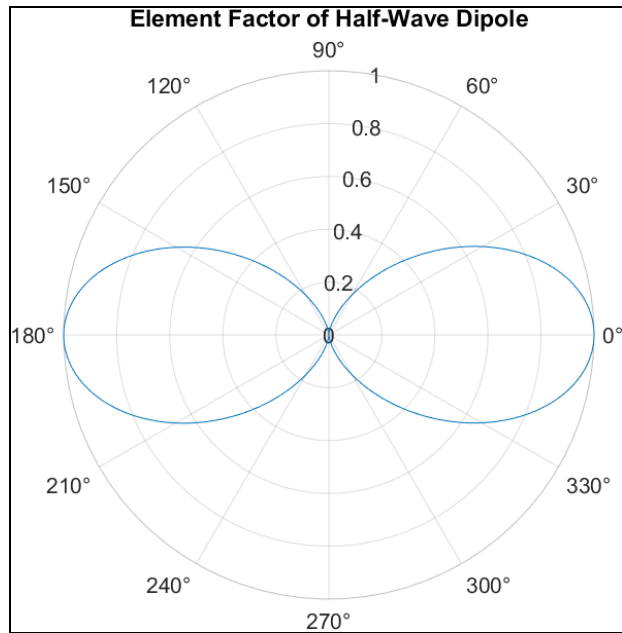


Figure 11: $\varphi=0$ degrees, 180 degrees

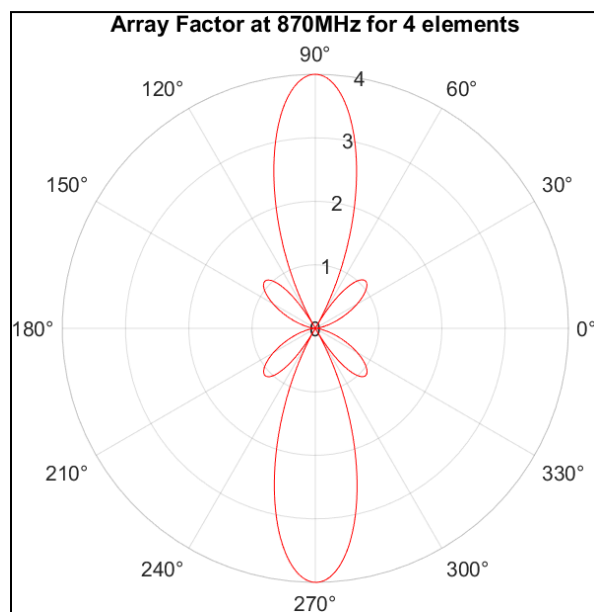


Figure 12: Plot of array factor for 4 elements along z-axis

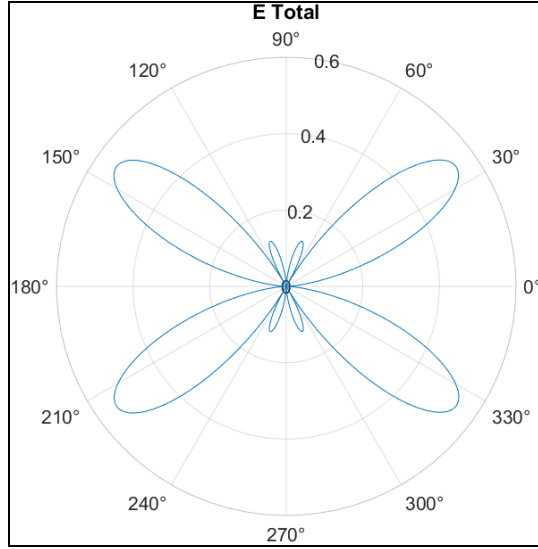


Figure 13: Total radiation pattern for dipoles parallel to x-axis arrayed along z

Nulls can be seen to occur at 0, 60, 90, 120, 180, 240, 270, and 300 degrees.

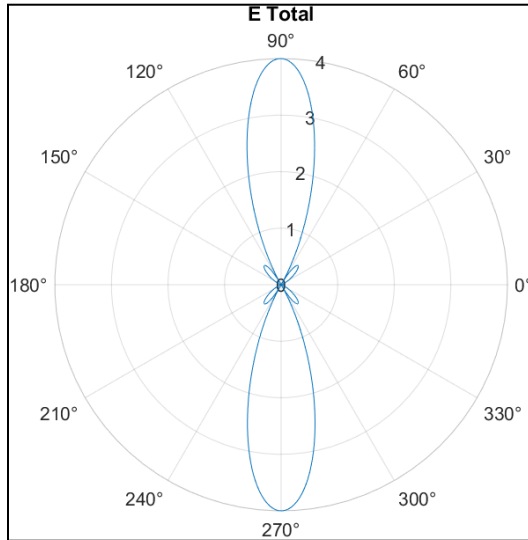


Figure 14: Total radiation pattern for dipoles parallel to z-axis along z

Nulls can be seen to occur at 0, 60, 90, 120, 180, 240, 270, and 300 degrees. (Same as *Figure 13*)

The radiation pattern in *Figure 9*, has a main lobe around 90° and 270° as expected in comparison to *Figure 14*, and in this way looks more similar to *Figure 14* than *Figure 13*. However, this could be attributed to measurement errors, since we notice the overall shape and number of main lobes more closely resembles *Figure 12*, consistent with theoretical expectations. We observe dips (nulls) along the 60° and 120° , creating 2 sidelobes on either side of the main lobe, which is consistent with our theoretical expectations from *Figures 13 and 14*.

4.2 Progressive Phase Shift with $\alpha = 90^\circ$

Table 5: S_{21} (dB) measurements for the four-element array with $d = \lambda/2$ and with progressive phase shift with $\alpha = 90^\circ$ with respect to various angles of rotation in 15 degree increments

Angle (in degrees)	S_{21} (dB)
0	-33
15	-29.5
30	-28.5
45	-28
60	-29
75	-31
90	-37
105	-34
120	-33
135	-32
150	-26.5
165	-26
180	-30
195	-26.5
210	-24
225	-22
240	-22.5
255	-25.5
270	-32
285	-31
300	-29
315	-31
330	-30.4
345	-33.3

Radiation Pattern of the Four-Element Array with $d = \lambda/2$ and $\alpha = 90^\circ$

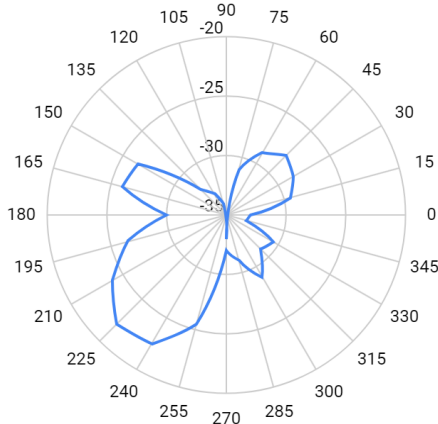


Figure 15: Co-polarized radiation pattern of the four-element antenna array with $d = \lambda/2$ and with progressive phase shift with $\alpha = 90^\circ$, plotted using the S21 (dB) measurements in Table 5

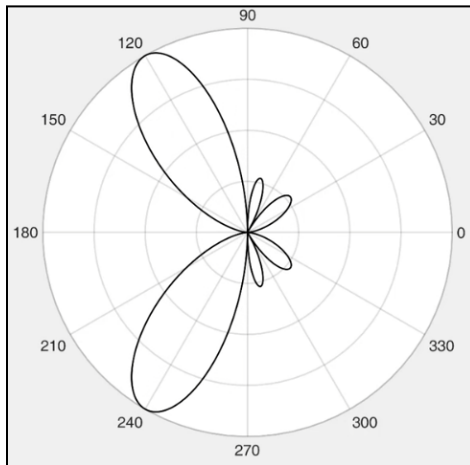


Figure 16: Theoretical radiation pattern of the four-element antenna array with $d = \lambda/2$ and $\alpha = 90^\circ$ [1]

$$\Psi = kdcos(\theta) + \alpha = \frac{2\pi}{\lambda} \frac{\lambda}{2} cos(\theta) + \frac{\pi}{2} = \pi cos(\theta) + \frac{\pi}{2}$$

\frac{N\Psi}{2} = \pm n\pi where $N = 4$ so that $\Psi = \pm \frac{n\pi}{2} = \pi cos(\theta) + \frac{\pi}{2}$

Nulls are expected to occur at $\theta = 0^\circ, 60^\circ, 90^\circ, 180^\circ$. We expect to observe a main beam along 120° as in Figure 16. The radiation pattern in Figure 15, has a main lobe around 240° as expected, although the main beam at 120° is not prominent. We observe nulls along the 90° and 180° which is consistent with our theoretical expectations from Figure 16. Although we don't observe 2 distinct sidelobes in the $(0^\circ, 90^\circ)$ range, we observe shapes that resemble 2 sidelobes along 300° and 330° , aligning with our expectations.

Calculate the expected beam angle (relative to broadside) and compare it to your measurements.

To determine the expected beam angle for a uniform linear array relative to broadside, the progressive phase shift α needs to compensate exactly for the phase difference due to path difference for radiation at angle θ from the array axis.

$$\alpha = kdsin(\theta)$$

$$\frac{\pi}{2} = \frac{2\pi}{\lambda} \frac{\lambda}{2} sin(\theta)$$

$$\frac{1}{2} = sin(\theta)$$

$$\theta = arcsin(\frac{1}{2}) = 30^\circ$$

Hence, we calculate the expected beam angle (relative to broadside) to be 30° , resulting in a main beam along 120° as seen in *Figure 16*.

In *Figure 15*, since we don't observe a prominent main beam in the $(90^\circ, 180^\circ)$ range, we can consider the main beam in the $(180^\circ, 270^\circ)$ range instead. By looking at the plot, we can approximate the beam angle to be $270^\circ - 240^\circ = 30^\circ$, which matches exactly to our expectations.

How would you reverse the beam angle so that it is steered on the opposite side of the broadside axis?

To reverse the beam angle, we need to reverse the direction of the progressive phase shift applied to the antenna elements. Therefore to steer the beam to the opposite side, we would apply a progressive phase shift of -90° .

$$\alpha = kdsin(\theta)$$

$$\theta = - 30^\circ$$

$$sin(- 30^\circ) = - \frac{1}{2}$$

$$\frac{2\pi}{\lambda} \frac{\lambda}{2} sin(- 30^\circ) = - \frac{\pi}{2}$$

5 Additional Questions

1. Classify each pattern obtained as either broadside, endfire, or other.

3.1. The first radiation pattern in *Figure 3* is broadside, and the radiation occurs perpendicular to the axis of the array.

3.2. The second radiation pattern in *Figure 5* is also broadside, with 2 significant sidelobes on each side of the main lobe.

3.3. The third radiation pattern in *Figure 7* demonstrates the endfire radiation pattern, with the main beam occurring on the same plane that contains the antenna array.

4.1. The fourth radiation pattern in *Figure 9* is broadside, with the main beam normal to the axis containing the antenna array and 2 sidelobes on each side.

4.2. The fifth radiation pattern in *Figure 15* is intermediate, in which the main beam is neither broadside or end-fire, but somewhere in between.

2. What is the approximate change in measured signal power from the array beam between the two-element array and the four-element array? Does it correspond to theoretical expectations?

The change in measured average signal power from the two-element array (-31.13 dB) to the four-element array (-29.85 dB) is an increase of approximately 1.28 dB. This increase aligns with our expectations, as adding more elements to the array generally increases both the total radiated power and the directivity of the array.

3. Explain how the patterns would have changed if the dipoles could have been mounted vertically (with the dipoles pointing along the same axis). Would it be possible to reconfigure each setup to realize this axial configuration? Why or why not?

As shown in Section 4.1, when all the elements are aligned along the z-axis instead of the x-axis, the array becomes much more directional as the number of main lobes reduces from 4 to 2.

If the dipoles could have been mounted vertically, the element factor would change shape accordingly. If we repositioned the elements to be along the meter stick, we would notice large gains at 90 and 270 degrees. If we mounted the meter stick vertically, we would be rotating about ϕ instead of θ . We would instead receive quite similar recordings from all directions, given the torus - like shape of the radiation pattern in three dimensions. We would not be able to glean information about the lobes and nulls in the pattern.

References

- [1] "Applied electromagnetic field theory chapter 32 -- Antenna Arrays," YouTube, <https://www.youtube.com/watch?v=9pov-HUWLiA> (accessed Feb. 21, 2024).
- [2] C. A. Balanis, *Antenna Theory: Analysis and Design.*, Page 292, Figure 6.4 Hoboken, NJ: Wiley, 2016.